

On the statistics of superlocalized states in self-affine disordered potentials

This article has been downloaded from IOPscience. Please scroll down to see the full text article.

2005 J. Phys. A: Math. Gen. 38 987

(<http://iopscience.iop.org/0305-4470/38/5/002>)

View [the table of contents for this issue](#), or go to the [journal homepage](#) for more

Download details:

IP Address: 171.66.16.94

The article was downloaded on 03/06/2010 at 04:05

Please note that [terms and conditions apply](#).

On the statistics of superlocalized states in self-affine disordered potentials

J M Luck

Service de Physique Théorique, URA 2306 of CNRS, CEA Saclay, 91191 Gif-sur-Yvette Cedex, France

E-mail: luck@spht.saclay.cea.fr

Received 6 September 2004

Published 19 January 2005

Online at stacks.iop.org/JPhysA/38/987

Abstract

We investigate the statistics of eigenstates in a weak self-affine disordered potential in one dimension, whose Gaussian fluctuations grow with distance with a positive Hurst exponent H . Typical eigenstates are superlocalized on samples much larger than a well-defined crossover length, which diverges in the weak-disorder regime. We present a parallel analytical investigation of the statistics of these superlocalized states in the discrete and the continuum formalisms. For the discrete tight-binding model, the effective localization length decays logarithmically with the sample size, and the logarithm of the transmission is marginally self-averaging. For the continuum Schrödinger equation, the superlocalization phenomenon has more drastic effects. The effective localization length decays as a power of the sample length, and the logarithm of the transmission is fully non-self-averaging.

PACS numbers: 71.23.An, 73.20.Fz, 72.15.Rn, 05.40.–a.

1. Introduction

The Anderson localization of a quantum-mechanical particle by a random potential is by now an old and well-understood problem [1]. This is especially so in one dimension. Consider for definiteness the tight-binding equation:

$$\psi_{n+1} + \psi_{n-1} + V_n \psi_n = E \psi_n. \quad (1.1)$$

In the usual situation where the site potentials V_n are uncorrelated, all the eigenstates are known to be exponentially localized (see, e.g., [2, 3]).

The peculiar features of the localization problem for various kinds of one-dimensional disordered potentials with non-trivial correlations have also been investigated, including dimer models [4], potentials with power-law correlations [5], potentials generated by chaotic dynamical systems [6], and potentials whose correlations are designed on purpose [7].

These examples share the common feature of *spatial stationarity*: the statistics of the potential is invariant under translation, so that its two-point correlation has a well-defined thermodynamical limit $\langle V_m V_n \rangle = C_{m-n}$, which only depends on the distance $|m - n|$.

The more exotic situation of *non-stationary* random potentials, whose fluctuations grow with distance, has only been considered more recently [8–13]. An example of most physical interest is that of a *self-affine* Gaussian potential with Hurst exponent $0 < H < 1$, such that

$$\langle (V_m - V_n)^2 \rangle = \Delta^2 |m - n|^{2H}. \quad (1.2)$$

Such a sequence of potentials can be generated by fractional Brownian motion, with a proper choice of stationary but correlated increments

$$\varepsilon_n = V_n - V_{n-1}. \quad (1.3)$$

The particular case of the usual Brownian motion, corresponding to stationary and independent increments ($\langle \varepsilon_m \varepsilon_n \rangle = \Delta^2 \delta_{mn}$), has a Hurst exponent $H = 1/2$.

An alternative way of characterizing non-stationary potentials consists in considering their structure factor $S(q) = \langle \hat{V}(q) \hat{V}(-q) \rangle$, assuming a power-law divergence of the form

$$S(q) \sim |q|^{-\alpha} \quad (1.4)$$

in the long-wavelength limit ($q \rightarrow 0$). Only the smaller values of the scaling exponent ($\alpha < 1$) correspond to stationary potentials, with long-range correlations falling off as $C_n \sim |n|^{-(1-\alpha)}$. Larger values of α necessarily correspond to non-stationary potentials. The above self-affine potentials with stationary increments are obtained in the range $1 < \alpha < 3$, with the correspondence $\alpha = 2H + 1$.

The main novel feature induced by the non-stationarity of the potential is that the effective disorder strength depends on the spatial scale. The typical potential fluctuation over a distance N indeed grows as $V_{\text{rms}}(N) = \Delta N^H$. It becomes therefore comparable with the bandwidth when the distance reaches the crossover length

$$N_{\text{cr}} = \Delta^{-1/H}. \quad (1.5)$$

The situation of most interest is that of a weak disorder ($\Delta \ll 1$), so that $N_{\text{cr}} \gg 1$. The eigenstates are conventionally localized on scales $N \ll N_{\text{cr}}$, with a localization length scaling as $\xi \sim 1/\Delta^2$. On larger scales ($N \gg N_{\text{cr}}$), however, eigenstates become strongly localized or *superlocalized* [12, 13], because wavefunctions fall off very fast in the classically forbidden zones of the potential ($|E - V_n| > 2$). Let us mention that an alternative viewpoint [8, 9] consists in keeping fixed the effective potential width $V_{\text{rms}}(N) = \Delta N^H = \Sigma$ at the scale of the system size N . The microscopic disorder strength $\Delta = \Sigma/N^H$ therefore gets rescaled to smaller and smaller values. The crossover length $N_{\text{cr}} = N/\Sigma^{1/H}$ grows proportionally to the sample size, whereas the localization length scales as $\xi \sim N^{2H}$. For a large enough non-stationarity ($H > 1/2$), such that ξ may become much larger than the sample size N , a crossover line in the (Σ, E) plane between extended and localized states has been observed [8, 9], and theoretically explained [12, 13].

The goal of the present work is to provide the first quantitative analysis of the statistics of superlocalized eigenstates, especially in the regime $N \gg N_{\text{cr}}$, where the superlocalization phenomenon is fully developed. We shall successively deal with the discrete tight-binding model (section 2) and the continuum Schrödinger equation (section 3).

The key quantity considered throughout this work is the effective Lyapunov exponent

$$\gamma_N = \frac{1}{N} \ln |\psi_N|, \quad (1.6)$$

where ψ_n is the generic (growing) solution to (1.1). The effective Lyapunov exponent provides an estimate of the global growth rate of this solution over N lattice sites, and therefore of the

effective decay rate of eigenstates over the same range. In other words, the effective localization length at scale N is

$$\xi_N = \frac{1}{\gamma_N}. \tag{1.7}$$

The effective Lyapunov exponent is also a central quantity in the theory of coherent quantum transport. Indeed the two-probe Landauer formula [14] expresses the zero-temperature conductance g_N of a sample made of N lattice sites, in terms of the intensity transmission T_N across that sample, as

$$g_N = \frac{2e^2}{h} T_N. \tag{1.8}$$

Furthermore, in the insulating regime where the transmission is small, it is known to scale as $T_N \sim 1/|\psi_N|^2$, hence

$$\ln T_N \approx -2N\gamma_N. \tag{1.9}$$

The effective Lyapunov exponent, and related physical quantities such as the effective localization length and the logarithm of the transmission (conductance), exhibit different kinds of scaling behaviour in the two situations to be investigated successively, the discrete tight-binding model (section 2) and the continuum Schrödinger equation (section 3). This basic difference is further commented on in the discussion (section 4).

2. The discrete tight-binding model

2.1. Reminder

We find it useful to first give a brief reminder on the conventional situation of a stationary random potential. The statistics of the size-dependent effective Lyapunov exponent γ_N is then very similar to that of the free-energy density of a disordered statistical-mechanical system [3, 15, 16]. The effective Lyapunov exponent γ_N has a well-defined self-averaging limit γ in the $N \rightarrow \infty$ limit, simply referred to as the Lyapunov exponent. Its reciprocal $\xi = 1/\gamma$ is interpreted as the localization length of the problem.

The fluctuations of γ_N around γ are Gaussian and scale as $\text{var } \gamma_N = \langle (\gamma_N - \gamma)^2 \rangle \approx \sigma^2/N$ for a finite but large enough sample ($N\gamma \gg 1$). More generally, the product $N\gamma_N$ is extensive, in the strong sense that all its cumulants

$$\langle\langle (N\gamma_N)^k \rangle\rangle \approx c_k N \tag{2.1}$$

grow linearly with N [3], with amplitudes $c_1 = \gamma$, $c_2 = \sigma^2$, and so on. It is worth noting that $N\gamma_N$, which is analogous to the total free energy, is also a physical observable in the present context, as it is nothing but the logarithm of the transmission (conductance), up to a constant factor [see (1.9)].

Furthermore, in the usual situation of independent site potentials with $\langle V_n \rangle = 0$ and $\langle V_m V_n \rangle = W^2 \delta_{mn}$, the Lyapunov exponent behaves as follows in the weak-disorder limit ($W^2 \ll 1$):

- Inside the band, i.e., for $|E| < 2$, setting $E = 2 \cos q$, the celebrated result [2]

$$\gamma \approx \frac{W^2}{8 \sin^2 q} = \frac{W^2}{2(4 - E^2)} \tag{2.2}$$

shows that the localization length diverges as $1/W^2$.

- Outside the band, i.e., for $|E| > 2$, setting $|E| = 2 \cosh t$, i.e.,

$$t = \ln \frac{|E| + \sqrt{E^2 - 4}}{2} > 0, \tag{2.3}$$

the generic solution to (1.1) grows exponentially as $\psi_n \sim e^{nt}$ in the absence of disordered potential, hence

$$\gamma \rightarrow t \quad (W^2 \rightarrow 0). \tag{2.4}$$

- Near band edges, i.e., for $E \rightarrow \pm 2$ and $W^2 \rightarrow 0$ simultaneously, the Lyapunov exponent obeys a scaling law of the form

$$\gamma \approx W^{2/3} F\left(\frac{|E| - 2}{W^{4/3}}\right), \tag{2.5}$$

where the scaling function F is explicitly known in terms of Airy functions [17].

2.2. General results

We now turn to the current problem, namely the tight-binding equation (1.1) with a weak self-affine potential whose fluctuations grow with distance according to (1.2), with $\Delta^2 \ll 1$. We choose the zero of energies as the site potential at the origin ($V_0 = 0$), and assume that the origin sits in an allowed zone, i.e., $|E| < 2$.

A long enough sample ($N \gg N_{cr}$) generically consists of an alternation of allowed zones ($|E - V_n| < 2$) and of forbidden zones ($|E - V_n| > 2$). It can be argued from the above results that the growth rate of a generic wavefunction is proportional to Δ^2 in allowed zones, i.e., inside the ‘local band’ around site n (where energies are shifted by V_n) [see (2.2)], whereas it is of order unity in forbidden zones, i.e., outside the ‘local band’ [see (2.4)].

This picture is fully corroborated by the plots shown in [12, 13], where eigenstates are indeed seen to be essentially constant in allowed zones, and to drop very suddenly in forbidden zones. Our main goal is to turn the above picture into a quantitative description of the statistics of the effective Lyapunov exponent (1.6).

Our starting point is the approximate formula

$$\psi_N \approx \exp\left(\sum_{n=0}^{N-1} t_n\right), \tag{2.6}$$

with the definition

$$E - V_n = 2 \cosh t_n, \tag{2.7}$$

hence

$$\gamma_N = \frac{1}{N} \sum_{n=0}^{N-1} \text{Re } t_n, \tag{2.8}$$

with

$$\text{Re } t_n = \begin{cases} \ln \frac{|E - V_n| + \sqrt{(E - V_n)^2 - 4}}{2} > 0 & \text{in forbidden zones } (|E - V_n| > 2), \\ 0 & \text{in allowed zones } (|E - V_n| < 2). \end{cases} \tag{2.9}$$

Let us first comment on (2.6) for a while. This expression is a full discrete analogue of the WKB integral (3.4), to be used in section 3. It provides a quantitative description of the growing solution to (1.1) in the forbidden zones of the potential, under the sole hypothesis that the sequence of site potentials has small increments:

$$\varepsilon_n = V_n - V_{n-1} \ll 1. \tag{2.10}$$

Expression (2.6) can be easily derived by introducing the Riccati variables [16, 18, 19]

$$R_n = \frac{\psi_{n+1}}{\psi_n}. \tag{2.11}$$

Assuming $\psi_0 = 1$, we have $\psi_n = R_0 \cdots R_{n-1}$, and

$$\gamma_N = \frac{1}{N} \sum_{n=0}^{N-1} \ln |R_n|. \tag{2.12}$$

The variables R_n obey the recursion

$$R_n = E - V_n - \frac{1}{R_{n-1}}. \tag{2.13}$$

If we now set

$$x_n = \frac{e^{t_n} - R_n}{1 - e^{t_n} R_n}, \quad R_n = \frac{e^{t_n} - x_n}{1 - e^{t_n} x_n}, \tag{2.14}$$

the variables x_n obey

$$x_n = e^{-2t_n} \frac{x_{n-1} + \delta_n}{1 + \delta_n x_{n-1}}, \tag{2.15}$$

with

$$\delta_n = \frac{e^{t_{n-1}} - e^{t_n}}{e^{t_n+t_{n-1}} - 1} \approx \frac{\varepsilon_n}{4 \sinh^2 t_n}, \tag{2.16}$$

to leading order as $\varepsilon_n \ll 1$. To the same order, the recursion (2.15) can be linearized to $x_n \approx e^{-2t_n} (x_{n-1} + \delta_n)$, implying that the x_n are proportional to the ε_n . One has therefore $R_n \approx \exp(t_n)$, up to terms proportional to the ε_n . Expressions (2.6) and (2.8) follow at once. Keeping track of higher powers of the ε_n in the above equations would be an efficient way of performing systematic weak-disorder expansions [16, 19].

Our analysis of the statistics of the effective Lyapunov exponent γ_N is based on the estimate (2.8). It turns out to be advantageous to introduce the Laplace representation

$$\text{Re } t_n = \int \frac{ds}{i\pi s} \cosh(sE) K_0(2s) \exp(sV_n), \tag{2.17}$$

where K_0 is the modified Bessel function, and the integration contour is a vertical line with $\text{Re } s > 0$. Using the Gaussian statistics of the potentials V_n , with $V_0 = 0$ and (1.2), we have

$$\langle \exp(sV_n) \rangle = \exp\left(\frac{1}{2} \Delta^2 s^2 n^{2H}\right), \tag{2.18}$$

and similar expressions for higher order characteristic functions such as $\langle \exp(s_1 V_m + s_2 V_n) \rangle$. We can therefore express the correlation functions of the variables $\text{Re } t_n$ as multiple contour integrals. By means of (2.8), the moments of the effective Lyapunov exponent γ_N can, in turn, be expressed as multiple integrals. The rescaling $x = m/N_{\text{cr}}$, $y = n/N_{\text{cr}}$ implies that, as could be expected, the final results only depend on the system size N through the dimensionless ratio

$$X = \frac{N}{N_{\text{cr}}} = \Delta^{1/H} N, \tag{2.19}$$

where the crossover scale N_{cr} has been introduced in (1.5). We thus obtain

$$\langle \gamma_N \rangle = \frac{1}{X} \int_0^X dx \int \frac{ds}{i\pi s} \cosh(sE) K_0(2s) \exp\left(\frac{1}{2} s^2 x^{2H}\right), \tag{2.20}$$

$$\langle \gamma_N^2 \rangle = \frac{1}{X^2} \int_0^X dx \int_0^X dy \int \frac{ds_1}{i\pi s_1} \cosh(s_1 E) K_0(2s_1) \int \frac{ds_2}{i\pi s_2} \cosh(s_2 E) K_0(2s_2) \times \exp\left(\frac{1}{2}(s_1^2 x^{2H} + s_1 s_2 (x^{2H} + y^{2H} - |x - y|^{2H}) + s_2^2 y^{2H})\right), \tag{2.21}$$

and so on.

The regimes of short samples ($N \ll N_{cr}$) and of long samples ($N \gg N_{cr}$) deserve to be considered separately.

2.3. Short samples

We first consider relatively short samples, such that $N \ll N_{cr}$, i.e., $X \ll 1$. In this regime, and for $|E| < 2$, the contour integral in (2.20) is dominated by a saddle point at $s_c \approx (2 - |E|)/x^{2H} \gg 1$. We thus obtain the following exponentially small estimate:

$$\langle \gamma_N \rangle \sim \exp\left(-\frac{(2 - |E|)^2}{2X^{2H}}\right) \tag{2.22}$$

for the mean effective Lyapunov exponent.

The right-hand side of (2.22) has a simple interpretation. It scales indeed as the probability that $E - V_N$ has reached the closest forbidden zone, i.e., $E - V_N = 2$ if $E > 0$ and $E - V_N = -2$ if $E < 0$, so that the superlocalization phenomenon just sets in.

For a weak but finite disorder strength Δ , the mean effective Lyapunov exponent $\langle \gamma_N \rangle$ is already of order Δ^2 in the regime of usual localization, i.e., for $X \ll 1$. The onset of superlocalization manifests itself as a crossover of $\langle \gamma_N \rangle$ to the behaviour (2.22), and it takes place for a system size such that

$$X \sim |\ln \Delta|^{-1/(2H)} \ll 1, \quad \text{i.e., } N \sim (\Delta |\ln \Delta|^{1/2})^{-1/H}. \tag{2.23}$$

2.4. Long samples

The superlocalization phenomenon is fully developed in the converse regime of long samples ($N \gg N_{cr}$, i.e., $X \gg 1$). The contour integral in (2.20) is then dominated by the branch cut of $K_0(2s) \approx -(\ln s + C)$ at $s = 0$, with C being Euler's constant. We thus obtain

$$\langle \gamma_N \rangle \approx H(\ln X - 1) - \frac{C + \ln 2}{2}. \tag{2.24}$$

The mean effective Lyapunov exponent thus diverges logarithmically with the system size N for $N \gg N_{cr}$, irrespective of the energy E .

As a matter of fact, the full distribution of the effective Lyapunov exponent simplifies in the limit of a long sample. Indeed, for $n \gg N_{cr}$ one has $\langle V_n^2 \rangle \gg 1$, so that most often $|V_n| \gg 1$, hence $\text{Re } t_n \approx \ln |V_n|$, and

$$\gamma_N \approx \frac{1}{N} \sum_{n=0}^{N-1} \ln |V_n|. \tag{2.25}$$

The rescaling $x = n/N$ yields the following asymptotic form of the effective Lyapunov exponent of long samples:

$$\gamma_N \approx H \ln X + G_H \approx H \ln(N/N_{cr}) + G_H \approx \ln(\Delta N^H) + G_H, \tag{2.26}$$

where the random additive term G_H is the following nonlinear functional of the normalized fractional Brownian motion:

$$G_H = \int_0^1 dx \ln |v(x)|. \tag{2.27}$$

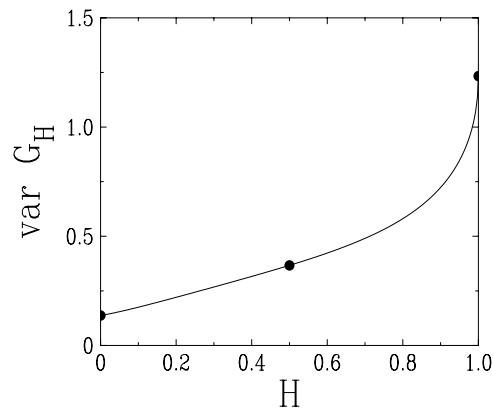


Figure 1. Plot of the variance of the functional G_H entering the result (2.26), evaluated from the exact expression (A.17), against the Hurst exponent H . Symbols: results (A.25), (A.27) and (A.30) for the particular cases $H = 0, 1/2$ and 1.

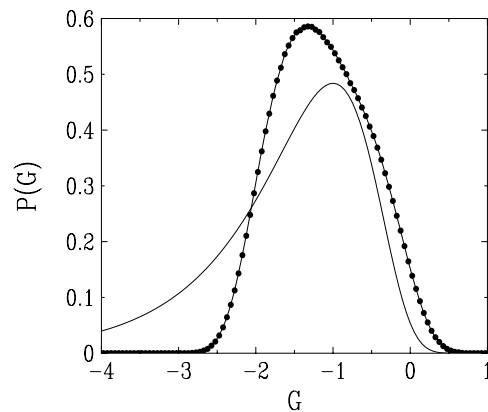


Figure 2. Plot of the probability density of the functional G_H entering the result (2.26). Thin full line: exact result (A.33) for $H = 1$ (ballistic limit). Line with symbols (showing histogram bins): numerical result for $H = 1/2$ (Brownian case).

Expression (2.26), which holds irrespectively of the energy E , is the main result of this section. The functional G_H is investigated in the appendix. It has a universal distribution which only depends on the Hurst exponent H . In the case $H = 1/2$, corresponding to usual Brownian motion, similar nonlinear integral functionals have been met in several physical problems [20]. To our knowledge, the distribution of G_H is not known explicitly, even in the Brownian case. Expressions for the mean and the variance of G_H are derived in the appendix for all H , as well as the full distribution of G_1 in the ballistic limit ($H = 1$). The mean $\langle G_H \rangle$ has a simple linear dependence (A.6) on the Hurst exponent H , which can already be read off from (2.24), while the more complex expression (A.17) for the variance $\text{var } G_H$ only simplifies for $H = 0, 1/2$, and 1. Figure 1 illustrates the dependence of $\text{var } G_H$ on the exponent H , whereas figure 2 shows a plot of the probability density of G_1 (ballistic case: exact expression (A.33)) and of $G_{1/2}$ (Brownian case), the latter being measured from an ensemble of numerically generated, and suitably rescaled, long random walks. The distributions is observed to be clearly asymmetric (skew), with very fast decaying tails at large values of G_H , and at small values of G_H for any $H < 1$.

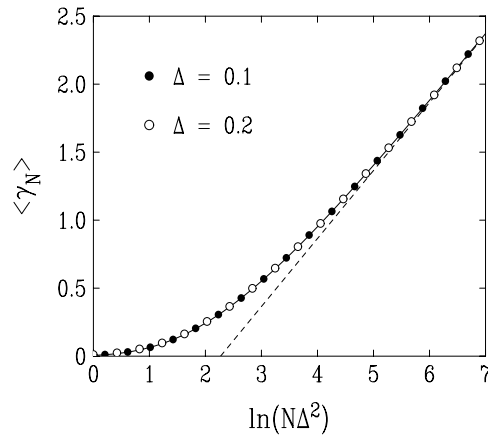


Figure 3. Plot of the mean effective Lyapunov exponent for a Brownian potential ($H = 1/2$) with $E = 0$, against the logarithm of the scaling variable $X = N\Delta^2$. Full curve: analytical prediction (2.20). Dashed line: asymptotic behaviour (2.24), i.e., $\langle \gamma_N \rangle \approx (\ln(N\Delta^2) - 1 - C - \ln 2)/2$. Symbols: numerical data for $\Delta = 0.1$ and $\Delta = 0.2$.

2.5. Numerical results

We have confronted our analytical predictions with numerical results in the Brownian case ($H = 1/2$). This situation is indeed simpler to handle than the generic one. On the one hand, the integrals over the rescaled spatial positions x, y in the predictions (2.20), (2.21) are elementary. On the other hand, sequences of Brownian potentials V_n can easily be generated numerically, by summing independent increments $\varepsilon_n = \pm\Delta$ with $\Delta \ll 1$, according to (1.3), with $V_0 = E = 0$.

The growing solution ψ_n has been evaluated by means of the recursion (2.13) for the Riccati variables R_n , with a random initial condition ($R_1 = \tan \phi$ with a uniform angle ϕ). The effective Lyapunov exponent has been measured by means of (2.12). The mean and the variance of the effective Lyapunov exponent are respectively shown in figures 3 and 4. The continuous curves represent the analytical results (2.20), (2.21), whereas symbols show numerical data for 10^5 samples with two strengths of disorder, $\Delta = 0.1$ and $\Delta = 0.2$. The accuracy of the data collapse and of the quantitative agreement with theoretical predictions provides a convincing check of our analysis.

3. The continuum Schrödinger equation

We now turn to the Schrödinger equation in a one-dimensional potential $V(x)$, which reads

$$-\psi''(x) + V(x)\psi(x) = E\psi(x), \quad (3.1)$$

in reduced units. The potential $V(x)$ is again assumed to be a weak self-affine Gaussian disordered potential with Hurst exponent $0 < H < 1$, such that

$$\langle (V(x) - V(y))^2 \rangle = \Delta^2 |x - y|^{2H}, \quad (3.2)$$

with $V(0) = 0$ and $\Delta^2 \ll 1$.

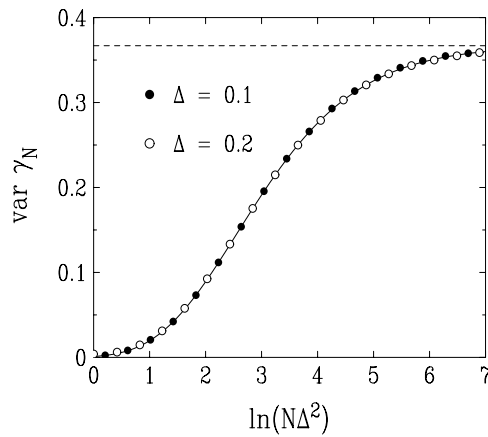


Figure 4. Plot of the variance of the effective Lyapunov exponent for a Brownian potential ($H = 1/2$) with $E = 0$, against the logarithm of the scaling variable $X = N\Delta^2$. Full curve: analytical prediction (2.21). Dashed line: limiting value (A.27): $\text{var } G_{1/2} = (\pi^2 - 4)/16 = 0.366850$. Symbols: numerical data for $\Delta = 0.1$ and $\Delta = 0.2$.

3.1. General results

The present situation shares most of the characteristic features of the tight-binding problem investigated in section 2. Its analysis will therefore only be described succinctly.

A long enough sample is again generically an alternation of classically allowed zones ($V(x) < E$) and of forbidden zones ($V(x) > E$). We assume $E > 0$, so that the origin belongs to an allowed zone. The growth rate of the generic solution of (3.1) up to distance L is measured by the effective Lyapunov exponent

$$\gamma(L) = \frac{1}{L} \ln|\psi(L)|. \tag{3.3}$$

The local growth rate of wavefunctions is again proportional to Δ^2 in allowed zones, whereas it is of order unity in forbidden zones. It is therefore legitimate to use the celebrated WKB integral (see e.g. [21, 22])

$$\psi(x) \sim \exp\left(\int_0^x dy \sqrt{(V(y) - E)_+}\right), \tag{3.4}$$

with the definition

$$\sqrt{(V(y) - E)_+} = \begin{cases} \sqrt{V(y) - E} & \text{in forbidden zones } (V(y) > E), \\ 0 & \text{in allowed zones } (V(y) < E). \end{cases} \tag{3.5}$$

The integral formula (3.4) provides a quantitative description, with exponential accuracy, of the growing solution to (3.1) in the forbidden zones of the potential, whenever the latter is slowly varying. One has therefore

$$\gamma(L) \approx \frac{1}{L} \int_0^L dx \sqrt{(V(x) - E)_+}. \tag{3.6}$$

Equations (3.6) and (3.5) are the continuum analogues of (2.8) and (2.9). They constitute the starting point of the subsequent analysis of the statistics of the effective Lyapunov exponent. It is again advantageous to introduce a Laplace representation:

$$\sqrt{(V(x) - E)_+} = \int \frac{ds}{2i\pi} \sqrt{\frac{\pi}{4s^3}} \exp(s(V(x) - E)). \tag{3.7}$$

The correlation functions of the variables $\sqrt{(V(x) - E)_+}$, and therefore the moments of the effective Lyapunov exponent, can again be expressed as explicit multiple integrals. We will only need the expression of the mean effective Lyapunov exponent, which reads

$$\langle \gamma(L) \rangle = \frac{1}{L} \int_0^L dx \int \frac{ds}{2i\pi} \sqrt{\frac{\pi}{4s^3}} \exp\left(\frac{1}{2} \Delta^2 s^2 x^{2H} - sE\right). \tag{3.8}$$

The rescalings $z = x/\ell_{cr}$, $u = sE$ show that the above result scales as

$$\langle \gamma(L) \rangle = \frac{E^{1/2}}{X} \int_0^X dz \int \frac{du}{2i\pi} \sqrt{\frac{\pi}{4u^3}} \exp\left(\frac{1}{2} u^2 z^{2H} - u\right), \tag{3.9}$$

in terms of the length ratio

$$X = \frac{L}{\ell_{cr}}, \tag{3.10}$$

where the energy-dependent crossover length

$$\ell_{cr} = (E/\Delta)^{1/H} \tag{3.11}$$

is the typical size of the first allowed zone containing the origin.

3.2. Short samples

For rather small samples, such that $L \ll \ell_{cr}$, i.e., $X \ll 1$, the contour integral in (3.9) is dominated by a saddle point at $u_c \approx z^{-2H} \gg 1$. We are thus left with the exponentially small estimate

$$\langle \gamma(L) \rangle \sim \exp\left(-\frac{1}{2X^{2H}}\right). \tag{3.12}$$

This expression again scales as the probability that $V(L)$ is equal to E , so that a forbidden zone has just been entered.

For a weak but finite disorder strength Δ , the mean effective Lyapunov exponent again has a finite limit of order Δ^2 for $X \ll 1$. The onset of superlocalization again takes place for a system size such that

$$X \sim |\ln \Delta|^{-1/(2H)} \ll 1, \quad \text{i.e.,} \quad L \sim \left(\frac{E}{\Delta |\ln \Delta|^{1/2}}\right)^{1/H}. \tag{3.13}$$

3.3. Long samples

The superlocalization phenomenon is fully developed in the converse regime of long samples ($L \gg \ell_{cr}$, i.e., $X \gg 1$). The contour integral in (3.9) is dominated by the square-root branch cut at $s = 0$. We thus obtain a power-law growth of the mean effective Lyapunov exponent:

$$\langle \gamma(L) \rangle \approx \frac{2^{1/4}}{(H+2)\sqrt{\pi}} \Gamma\left(\frac{3}{4}\right) (\Delta L^H)^{1/2}, \tag{3.14}$$

irrespective of the energy E .

The full distribution of the effective Lyapunov exponent again simplifies in the limit of a long sample. Indeed, for $x \gg \ell_{cr}$, E is most often negligible with respect to $V(x)$. Equation (3.6) therefore simplifies to

$$\gamma(L) \approx \frac{1}{L} \int_0^L dx \sqrt{(V(x))_+}. \tag{3.15}$$

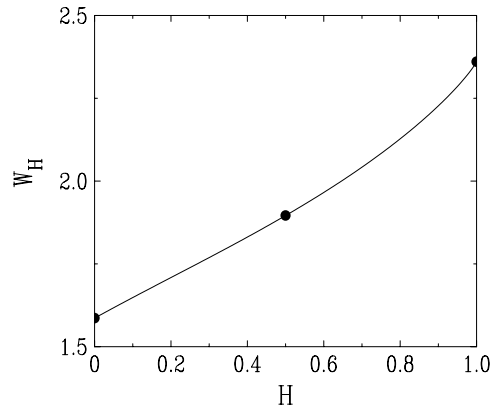


Figure 5. Plot of the moment ratio W_H , defined in (3.18), of the quantity Y_H entering the result (3.16), evaluated from the exact expression (A.23), against the Hurst exponent H . Symbols: results (A.25), (A.28) and (A.30) for the particular cases $H = 0, 1/2$ and 1 .

The rescaling of x by L yields the following asymptotic form of the effective Lyapunov exponent of long samples:

$$\gamma(L) \approx E^{1/2} X^{H/2} Y_H \approx E^{1/2} (L/\ell_{cr})^{H/2} Y_H \approx (\Delta L^H)^{1/2} Y_H, \tag{3.16}$$

where the fluctuating factor Y_H is another nonlinear functional of the normalized fractional Brownian motion:

$$Y_H = \int_0^1 dx \sqrt{(v(x))_+}. \tag{3.17}$$

This functional is investigated in the appendix. It has a universal distribution which only depends on the Hurst exponent H . Its first two moments are evaluated for all values of H (see respectively (A.6) and (A.22)), as well as the full distribution of Y_1 in the ballistic limit. Figure 5 illustrates the dependence of the dimensionless ratio

$$W_H = \frac{\langle Y_H^2 \rangle}{\langle Y_H \rangle^2} \tag{3.18}$$

on the exponent H . Figure 6 shows a plot of the probability density of Y_1 (ballistic case: exact expression (A.33)) and of $Y_{1/2}$ (Brownian case), the latter being measured from an ensemble of numerically generated, and suitably rescaled, long random walks. The delta peak at $Y = 0$, which is present in the ballistic limit ($H = 1$), gets smeared out into a continuous density which diverges as $Y \rightarrow 0$ for any $H < 1$.

4. Discussion

The present work is devoted to the specific features of localization in a weak self-affine disordered potential in one dimension, whose fluctuations grow with distance with a positive Hurst exponent H . The most salient feature of such non-stationary potentials is that the effective disorder strength depends on the spatial scale. Even in the regime of most physical interest, where the fluctuations of the disordered potential are small at the microscopic scale ($\Delta \ll 1$), the effective disorder becomes strong beyond a well-defined crossover length N_{cr} or ℓ_{cr} , which diverges as $\Delta^{-1/H}$. Samples much longer than this crossover length typically consist of an alternation of classically allowed zones, where the growth rate of a generic wavefunction is

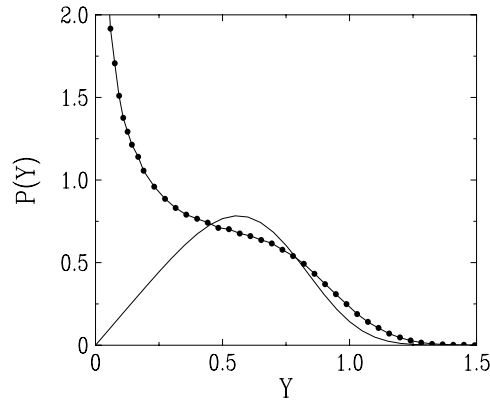


Figure 6. Plot of the probability density of the random variable Y_H entering the result (3.16). Thin full line: continuous component (delta peak at $Y = 0$ omitted) of the exact result (A.33) for $H = 1$ (ballistic limit). Line with symbols (showing histogram bins): numerical result for $H = 1/2$ (Brownian case).

small and proportional to the square disorder strength Δ^2 , and of forbidden zones, where this growth rate is large. Typical eigenstates on such samples turn out to be superlocalized [12, 13].

In this paper we present a parallel analytical investigation of the statistics of superlocalized eigenstates, for both the discrete tight-binding model and the continuum Schrödinger equation. First of all, the clear separation of the growth rates of wavefunctions in allowed and in forbidden zones in the weak-disorder regime is shown to allow for a semi-classical treatment of the superlocalization phenomenon, by means of the WKB formalism. The key quantity is the size-dependent effective Lyapunov exponent, which is closely related to the transmission across the sample, and therefore to its zero-temperature conductance by the Landauer formula.

For the discrete tight-binding model, investigated in section 2, the effective Lyapunov exponent behaves as

$$\gamma_N \approx H \ln(N/N_{\text{cr}}) + G_H \approx \ln(\Delta N^H) + G_H \quad (4.1)$$

in the fully superlocalized regime of long samples ($N \gg N_{\text{cr}}$) [see (2.26)]. The fluctuating part G_H is an *additive term* of order unity. It is given by the functional (2.27), whose limit distribution only depends on the Hurst exponent H . These results translate as follows in terms of physical quantities. One of the most characteristic features of superlocalization is the fall-off of the effective localization length ξ_N as a function of N . This decay is however only logarithmic, as $\xi_N \approx 1/[H \ln(N/N_{\text{cr}})]$. As far as the transmission T_N is concerned (or equivalently the conductance g_N), the relevant quantity is its logarithm, as in most localization problems. Its mean grows as $\langle \ln T_N \rangle \approx -2HN \ln(N/N_{\text{cr}})$, whereas its variance grows as $\text{var} \ln T_N \approx 4 \text{var} G_H N^2$. The logarithm of the transmission is therefore *marginally self-averaging*, as its relative variance $\text{var} \ln T_N / \langle \ln T_N \rangle^2 \sim 1/[\ln(N/N_{\text{cr}})]^2$ falls off logarithmically.

For the continuum Schrödinger equation, investigated in section 3, the effective Lyapunov exponent behaves as

$$\gamma(L) \approx E^{1/2}(L/\ell_{\text{cr}})^{H/2} Y_H \approx (\Delta L^H)^{1/2} Y_H \quad (4.2)$$

[see (3.16)] in the fully superlocalized regime. The fluctuating part Y_H of this result, given by the functional (3.17), is now involved *as a multiplicative factor*. This multiplicative law generates more pronounced superlocalization effects, and especially stronger fluctuations in

Table 1. Scaling behaviour of various quantities in the regime of fully developed superlocalization: mean effective localization length, mean and relative variance of the logarithm of the transmission (conductance). Only the qualitative scaling behaviour is given (dependence on the sample size N or L and on the disorder strength Δ). The emphasis is put on the difference between the discrete tight-binding model (additive fluctuation in the effective Lyapunov exponent) and the continuum Schrödinger equation (multiplicative fluctuation). The well-known results for conventional Anderson localization are recalled for comparison.

Quantity	Tight-binding model $N \gg N_{\text{cr}}$ sites	Schrödinger equation length $L \gg \ell_{\text{cr}}$	Anderson localization
$\langle \xi \rangle$	$1/\ln(N/N_{\text{cr}})$	$(\Delta L^H)^{-1/2}$	$1/\Delta^2$
$-\langle \ln T \rangle$	$N \ln(N/N_{\text{cr}})$	$\Delta^{1/2} L^{1+H/2}$	$\Delta^2 L$
$\text{var} \ln T / (\ln T)^2$	$1/[\ln(N/N_{\text{cr}})]^2$	Constant	$1/(\Delta^2 L)$

physical quantities. The effective localization length $\xi(L) \approx 1/(Y_H \Delta^{1/2} L^{H/2})$ now decays as a power of the sample length, with a fluctuating amplitude. As far as the transmission is concerned, its mean grows as $\langle \ln T(L) \rangle \sim -\Delta^{1/2} L^{1+H/2}$, i.e., more rapidly than linearly with the sample length. The logarithm of the transmission is now *fully non-self-averaging*, as its relative variance $\text{var} \ln T(L) / (\ln T(L))^2 \rightarrow W_H - 1$ has a non-trivial limit for $L \gg \ell_{\text{cr}}$.

The effective Lyapunov exponent and related physical quantities therefore exhibit two different kinds of statistics in the discrete and in the continuum formalism. The basic difference between both situations is already present in the case of a constant potential. It is indeed deeply rooted in the dispersion relations of the models. For the tight-binding model with a constant site potential V outside the band, the growth rate t of wavefunctions is such that $E - V = 2 \cosh t$, and therefore only diverges logarithmically as $t \approx \ln|V|$ for large V . For the continuum Schrödinger equation with a constant potential V , the growth rate now obeys $V - E = t^2$, and diverges as $t \approx \sqrt{V}$. Replacing in the above dispersion estimates t by γ , and V by the product of a random number of order unity by $V_{\text{rms}} \sim \Delta N^H$ or ΔL^H , leads to the correct qualitative forms of the scaling equations (4.1) and (4.2). Finally, this line of reasoning also shows that the results for the Schrödinger equation cannot be recovered from those of the tight-binding model by going to the continuum limit, because this limit corresponds to $t \rightarrow 0$, whereas superlocalization is essentially due to large values of t . Table 1 summarizes the discussion.

Let us close with a word on the generality of our results. For any weak self-affine (not necessarily Gaussian) random potential obeying power laws of the form (1.2) or (3.2), with any positive Hurst exponent H , both the functional form of the results (4.1), (4.2) and the scaling laws recalled in table 1 can be shown to still hold true. The fluctuating parts G_H and Y_H are, however, only given by (2.27) and (3.17) for the Gaussian self-affine potentials associated with fractional Brownian motion. Their distribution involve in general further details of the statistics of the potentials.

Acknowledgments

It is a pleasure to thank Dominique Boosé for very stimulating discussions.

Appendix. The functionals G_H and Y_H

This appendix is devoted to the random quantities G_H and Y_H , which respectively enter our key results (2.26) and (3.16). They are defined as the following nonlinear functionals:

$$G_H = \int_0^1 dx \ln|v(x)|, \quad Y_H = \int_0^1 dx \sqrt{(v(x))_+}, \quad (\text{A.1})$$

of the normalized fractional Brownian motion $v(x)$ with Hurst exponent $0 < H < 1$ on $0 \leq x \leq 1$, so that $v(0) = 0$ and

$$\langle (v(x) - v(y))^2 \rangle = |x - y|^{2H}. \quad (\text{A.2})$$

First moments. The means (first moments)

$$\langle G_H \rangle = \int_0^1 dx \langle \ln|v(x)| \rangle, \quad \langle Y_H \rangle = \int_0^1 dx \langle \sqrt{(v(x))_+} \rangle, \quad (\text{A.3})$$

can be readily evaluated. Indeed, $v(x)$ is a Gaussian with variance $\langle v(x)^2 \rangle = x^{2H}$, so that its probability density reads

$$P(v(x)) = \frac{1}{x^H \sqrt{2\pi}} \exp\left(-\frac{v(x)^2}{2x^{2H}}\right). \quad (\text{A.4})$$

Elementary integrals yield

$$\langle \ln|v(x)| \rangle = H \ln x - \frac{\mathbf{C} + \ln 2}{2}, \quad \langle \sqrt{(v(x))_+} \rangle = \frac{1}{2^{3/4} \sqrt{\pi}} \Gamma\left(\frac{3}{4}\right) x^{H/2}, \quad (\text{A.5})$$

so that

$$\langle G_H \rangle = -H - \frac{\mathbf{C} + \ln 2}{2}, \quad \langle Y_H \rangle = \frac{2^{1/4}}{(H+2)\sqrt{\pi}} \Gamma\left(\frac{3}{4}\right). \quad (\text{A.6})$$

Second moments. The second moments

$$\langle G_H^2 \rangle = 2 \int_0^1 dx \int_x^1 dy \langle \ln|v(x)| \ln|v(y)| \rangle, \quad \langle Y_H^2 \rangle = 2 \int_0^1 dx \int_x^1 dy \langle \sqrt{(v(x))_+ (v(y))_+} \rangle, \quad (\text{A.7})$$

now involve two-point observables, expressed in terms of the correlated Gaussian variables $v(x)$ and $v(y)$, such that

$$\langle v(x)^2 \rangle = x^{2H}, \quad \langle v(y)^2 \rangle = y^{2H}, \quad \langle v(x)v(y) \rangle = \frac{1}{2}(x^{2H} + y^{2H} - (y-x)^{2H}). \quad (\text{A.8})$$

It is convenient to use polar coordinates in the $v(x), v(y)$ plane. For $x \leq y$, we set

$$z = \frac{x}{y} \leq 1, \quad (\text{A.9})$$

and

$$v(x) = r \cos \theta, \quad v(y) = \frac{r}{z^H} \sin(\theta + \alpha), \quad (\text{A.10})$$

with

$$\sin \alpha = \frac{\langle v(x)v(y) \rangle}{\sqrt{\langle v(x)^2 \rangle \langle v(y)^2 \rangle}} = \frac{1 + z^{2H} - (1-z)^{2H}}{2z^H} \quad (0 \leq \alpha \leq \pi/2). \quad (\text{A.11})$$

This parametrization ensures that the angle θ is uniformly distributed between 0 and 2π , whereas the radial variable r has a probability density

$$P_r(r) = \frac{r}{x^{2H}} \exp\left(-\frac{r^2}{2x^{2H}}\right). \quad (\text{A.12})$$

The calculation of $\langle \ln|v(x)| \ln|v(y)| \rangle$ splits into the radial integrals

$$\langle \ln r \rangle = \frac{\ln(2x^{2H}) - \mathbf{C}}{2}, \quad \langle (\ln r)^2 \rangle_c = \frac{\pi^2}{24}, \quad (\text{A.13})$$

where $\langle \dots \rangle_c$ denotes the connected part, and the angular integrals

$$\langle \ln|\cos \theta| \rangle = \langle \ln|\sin \theta| \rangle = -\ln 2, \quad \langle \ln|\cos(\theta)|\ln|\sin(\theta + \alpha)| \rangle_c = \frac{\alpha^2}{2} - \frac{\pi^2}{24}. \quad (\text{A.14})$$

The derivation of the second result requires the use of the Fourier series

$$\sum_{n=1}^{\infty} (-1)^n \frac{\cos(2n\theta)}{n} = -\ln(2|\cos \theta|), \quad \sum_{n=1}^{\infty} (-1)^n \frac{\cos(2n\theta)}{n^2} = \theta^2 - \frac{\pi^2}{12}, \quad (\text{A.15})$$

where the latter equality holds for $|\theta| \leq \pi$. We thus obtain the following simple expression:

$$\langle \ln|v(x)|\ln|v(y)| \rangle_c = \frac{\alpha^2}{2} \quad (\text{A.16})$$

for the connected correlation function, which leads us to the result

$$\text{var } G_H = \langle G_H^2 \rangle_c = \frac{1}{2} \int_0^1 \alpha^2 dz, \quad (\text{A.17})$$

where α is defined in terms of z by (A.11).

Similarly, the calculation of $\langle \sqrt{(v(x))_+(v(y))_+} \rangle$ splits into the radial integral

$$\langle r \rangle = \sqrt{\frac{\pi}{2}} x^H, \quad (\text{A.18})$$

and the angular integral

$$\int_{-\alpha}^{\pi/2} \frac{d\theta}{2\pi} \sqrt{\cos \theta \sin(\theta + \alpha)} = \frac{k^2}{\pi} \int_0^{\pi/2} \frac{\cos^2 \phi d\phi}{\sqrt{1 - k^2 \sin^2 \phi}} = \frac{1}{\pi} (\mathbf{E}(k) - (1 - k^2)\mathbf{K}(k)), \quad (\text{A.19})$$

where we have set

$$\sin\left(\theta + \frac{\alpha}{2} - \frac{\pi}{4}\right) = k \sin \phi, \quad (\text{A.20})$$

with

$$k^2 = \sin^2\left(\frac{\pi}{4} + \frac{\alpha}{2}\right) = \frac{1 + \sin \alpha}{2} = \frac{(1 + z^H)^2 - (1 - z)^{2H}}{4z^H}, \quad (\text{A.21})$$

and where $\mathbf{E}(k)$ and $\mathbf{K}(k)$ are complete elliptic integrals. Finally,

$$\langle Y_H^2 \rangle = \frac{1}{H + 2} \sqrt{\frac{2}{\pi}} \int_0^1 (\mathbf{E}(k) - (1 - k^2)\mathbf{K}(k)) z^{H/2} dz, \quad (\text{A.22})$$

so that

$$W_H = \frac{\langle Y_H^2 \rangle}{\langle Y_H \rangle^2} = \frac{H + 2}{2\pi^{3/2}} \Gamma\left(\frac{1}{4}\right)^2 \int_0^1 (\mathbf{E}(k) - (1 - k^2)\mathbf{K}(k)) z^{H/2} dz, \quad (\text{A.23})$$

where k is defined in terms of z by (A.21).

The general expressions (A.17) and (A.23) simplify in the following particular cases.

Ultraslow limit ($H = 0$). In this limit we have

$$\alpha = \frac{\pi}{6}, \quad k = \frac{\sqrt{3}}{2}, \quad (\text{A.24})$$

irrespective of z , hence

$$\begin{aligned} \text{var } G_0 &= \frac{\pi^2}{72} = 0.137\,078, \\ W_0 &= \frac{1}{\pi^{3/2}} \Gamma\left(\frac{1}{4}\right)^2 \left(\mathbf{E}\left(\frac{\sqrt{3}}{2}\right) - \frac{1}{4} \mathbf{K}\left(\frac{\sqrt{3}}{2}\right) \right) = 1.586\,206. \end{aligned} \quad (\text{A.25})$$

Brownian case ($H = 1/2$). In this case we have

$$\sin \alpha = 2k^2 - 1 = \sqrt{z}, \quad (\text{A.26})$$

so that a direct integration yields

$$\text{var } G_{1/2} = \frac{\pi^2 - 4}{16} = 0.366\,850. \quad (\text{A.27})$$

In order to evaluate $W_{1/2}$, it is more convenient to go back to the middle expression of (A.19), and to integrate first over k , then over ϕ . We thus obtain after some algebra

$$W_{1/2} = \frac{5}{288\pi^{3/2}} \Gamma\left(\frac{1}{4}\right)^2 (50 - 3\sqrt{2}\ln(1 + \sqrt{2})) = 1.895\,949. \quad (\text{A.28})$$

Ballistic limit ($H = 1$). In this case we have

$$\alpha = \frac{\pi}{2}, \quad k = 1, \quad (\text{A.29})$$

irrespective of z , hence

$$\text{var } G_1 = \frac{\pi^2}{8} = 1.233\,701, \quad W_1 = \frac{1}{\pi^{3/2}} \Gamma\left(\frac{1}{4}\right)^2 = 2.360\,681. \quad (\text{A.30})$$

The constancy of $\alpha = \pi/2$ means that $v(x)$ and $v(y)$ are fully correlated. Their correlation functions (A.8) indeed saturate the Cauchy–Schwarz inequality.

The whole fractional Brownian process degenerates into a one-variable problem in the ballistic limit. We have indeed

$$v(x) = xw, \quad (\text{A.31})$$

where $w \equiv v(1)$ is a Gaussian variable such that $\langle w^2 \rangle = 1$, hence

$$G_1 = \ln|w| - 1, \quad Y_1 = \frac{2}{3}\sqrt{w_+}. \quad (\text{A.32})$$

By performing the appropriate changes of variables on the Gaussian law of w , we get the following explicit expressions for the probability densities:

$$P(G_1) = \sqrt{\frac{2}{\pi}} \exp\left(G_1 + 1 - \frac{1}{2}e^{2(G_1+1)}\right), \quad P(Y_1) = \frac{1}{2}\delta(Y_1) + \frac{9Y_1}{2\sqrt{2\pi}} \exp\left(-\frac{81Y_1^4}{32}\right). \quad (\text{A.33})$$

References

- [1] See e.g., Lifshitz I M, Gredeskul S A and Pastur L A 1988 *Introduction to the Theory of Disordered Systems* (New York: Wiley)
Kramer B and MacKinnon A 1993 *Rep. Prog. Phys.* **56** 1469
Imry Y 1997 *Introduction to Mesoscopic Physics* (Oxford: Oxford University Press)
Efetov K 1997 *Supersymmetry in Disorder and Chaos* (Cambridge: Cambridge University Press)
- [2] Thouless D J 1979 La matière mal condensée: III Condensed matter *Proc. Les Houches Summer School* ed R Balian, R Maynard and G Toulouse (Amsterdam: North-Holland)
- [3] Pendry J B 1994 *Adv. Phys.* **43** 461
- [4] Dunlap D H, Wu H L and Phillips P W 1990 *Phys. Rev. Lett.* **65** 88
- [5] Russ S, Havlin S and Webman I 1998 *Phil. Mag.* B **77** 1449
Russ S 2002 *Phys. Rev. B* **66** 012204
de Moura F A B F, Coutinho-Filho M D, Raposo E P and Lyra M L 2003 *Phys. Rev. B* **68** 012202

- [6] Yamada H, Goda M and Aizawa Y 1991 *J. Phys.: Condens. Matter.* **3** 10043
Yamada H, Goda M and Aizawa Y 1991 *J. Phys. Soc. Japan* **60** 3501
Pinto R A, Rodriguez M, Gonzalez J A and Medina E 2004 *Preprint* cond-mat/0402364
- [7] Izrailev F M and Krokhnin A A 1999 *Phys. Rev. Lett.* **82** 4062
Izrailev F M, Krokhnin A A and Ulloa S E 2001 *Phys. Rev. B* **63** 041102
Tessieri L 2002 *J. Phys. A: Math. Gen.* **35** 9585
- [8] de Moura F A B F and Lyra M L 1998 *Phys. Rev. Lett.* **81** 3735
- [9] de Moura F A B F and Lyra M L 1999 *Physica A* **266** 465
- [10] Kantelhardt J W, Russ S, Bunde A, Havlin S and Webman I 2000 *Phys. Rev. Lett.* **84** 198
- [11] de Moura F A B F and Lyra M L 2000 *Phys. Rev. Lett.* **84** 199
- [12] Bunde A, Havlin S, Kantelhardt J W, Russ S and Webman I 2000 *J. Mol. Liq.* **86** 151
- [13] Russ S, Kantelhardt J W, Bunde A and Havlin S 2001 *Phys. Rev. B* **64** 134209
- [14] Imry Y and Landauer R 1999 *Rev. Mod. Phys.* **71** S306
- [15] Crisanti A, Paladin G and Vulpiani A 1992 *Products of Random Matrices in Statistical Physics* (Berlin: Springer)
- [16] Luck J M 1992 *Systèmes Désordonnés Unidimensionnels (in French) (Collection Aléa-Saclay)*
- [17] Derrida B and Gardner E 1984 *J. Physique* **45** 1283
- [18] Nieuwenhuizen M Th 1982 *Physica A* **113** 173
- [19] Luck J M 1989 *Phys. Rev. B* **39** 5834
- [20] Monthus C and Comtet A 1994 *J. Physique I* **4** 635
Monthus C 1995 *Ann. Phys., Paris* **20** 341
Comtet A, Monthus C and Yor M 1998 *J. Appl. Probab.* **35** 255
Majumdar S N and Comtet A 2004 *Phys. Rev. Lett.* **92** 225501
- [21] Landau L D and Lifshitz E M 1959 *Quantum Mechanics: Non-Relativistic Theory* (Oxford: Pergamon)
- [22] Fröman N and Fröman P O 2002 *Physical Problems Solved by the Phase-Integral Method* (Cambridge: Cambridge University Press)